

# Optimizing a Boundary Elements Method for Stationary Elastodynamic Problems implementation with GPUs

Giuliano A. F. Belinassi<sup>1</sup>, Rodrigo Siqueira<sup>1</sup>, Ronaldo Carrion<sup>2</sup>, Alfredo Goldman<sup>1</sup>,  
Marco D. Gubitoso<sup>1</sup>

<sup>1</sup>Instituto de Matemática e Estatística (IME) – Universidade de São Paulo (USP)  
Rua do Matão, 1010 – São Paulo – SP – Brazil

<sup>2</sup>Escola Politécnica (EP) – Universidade de São Paulo (USP)  
Avenida Professor Mello Moraes, 2603 – São Paulo – SP – Brazil

**Abstract.** *The Boundary Element Method requires a geometry discretization to execute simulations, and it can be used to analyze the 3D stationary behavior of wave propagation in the soil. Such discretization involves generating two high computational power demanding matrices, and this article demonstrates how Graphical Processing Units (GPU) were used to accelerate this process. For an experiment with 4000 Mesh elements and 1600 Boundary elements, a speedup of  $107\times$  was obtained with a GeForce GTX980.*

## 1. Introduction

Differential equations governing problems of Mathematical Physics only have analytical solutions in cases in which the domain geometry, boundary and initial conditions are reasonably simple. Problems with arbitrary domains and fairly general boundary conditions are only solved with an approximation artifice, for example, by numerical techniques. These techniques were strongly developed due to the presence of increasingly powerful computers, allowing the solution of complex mathematical problems.

The Boundary Element Method (BEM) is a very efficient alternative for modeling unlimited domains since it naturally satisfies the Sommerfeld radiation condition, also known as geometric damping [Katsikadelis 2016]. Such method can be used for numerically modeling the 3D stationary behavior of wave propagation in the soil, it is useful as a computation tool to aid in the analysis of soil vibration [Dominguez 1993]. A BEM based tool can be used for analyzing the vibration created by heavy machines, railway lines, earthquakes, or even to aid the design of offshore oil platforms.

With the advent of GPUs, several mathematical and engineering simulation problems were redesigned to be implemented into these massively parallel devices. However, first GPUs were designed to render graphics in real time, as a consequence, all the available libraries were graphical oriented such as OpenGL. These redesigns involved converting the original problem into a graphical domain, requiring deep knowledge of the selected graphical library.

NVIDIA noticed a new demand for their products and created an API called CUDA to enable the use of GPUs in general purpose situations. CUDA has the concept of kernels, which are functions called from host to be executed by the GPU threads. Kernels are organized into a set of blocks wherein each block is a set of threads that cooperate with each other [Patterson and Hennessy 2007].

GPU's memory is divided into global memory, local memory, and shared memory. First, it is a memory that all threads can access. Second, it is a memory that is private to a thread. Third, it is a low-latency memory that is shared between all threads in the same block [Patterson and Hennessy 2007]. CUDA provides mechanisms to access all of them.

Regarding this work, this parallelization approach is useful because an analysis of a large domain requires a proportionally large number of mesh elements, and processing a single mesh have a high time cost. Doing such analysis in parallel reduces the computational time required for the entire program because multiple meshes are processed at the same time. This advantage was provided by this research.

Before discussing any parallelization technique or results, Section 2 presents a very brief mathematical formulation of BEM for Stationary Elastodynamic Problems and the meaning of some functions presented in the current work. Section 3 shows how the most computational expensive routine was optimized using GPUs. Section 4 discusses how the results were obtained. Section 5 presents and discusses the results. Finally, Section 6 provides an overview of our future work.

## 2. Boundary Elements Method Background

Without addressing details on BEM formulation, the Boundary Integral Equation for Stationary Elastodynamic Problems can be written as:

$$c_{ij}u_j(\xi, \omega) + \int_S t_{ij}^*(\xi, x, \omega)u_j(x, \omega)dS(x) = \int_S u_{ij}^*(\xi, x, \omega)t_j(x, \omega)dS(x) \quad (1)$$

After performing the geometry discretization, Equation (1) can be represented in matrix form as:

$$Hu = Gt \quad (2)$$

Functions  $u_{ij}^*(\xi, x, \omega)$  and  $t_{ij}^*(\xi, x, \omega)$  (called fundamental solutions) present a singular behavior when  $\xi = x$  ordely  $O(1/r)$ , called weak singularity, and  $O(1/r^2)$ , called strong singularity, respectively. The  $r$  value represents the distance between  $x$  and  $\xi$  points. Integral of these functions, as represented in Eq. (1), will generate  $G$  and  $H$  matrices respectively showed in Eq. (2). For computing these integrals numerically, the Gaussian quadrature can be deployed. Briefly, it is an algorithm that approximates integrals by sums as shown in equation (3)[Ascher and Greif 2011], where  $g$  is the number of Gauss quadrature points.

$$\int_a^b f(x)dx \approx \sum_{i=1}^g w_i f(x_i) \quad (3)$$

To overcome the mentioned problem in the strong singularity, ones use the artifice known as Regularization of the Singular Integral that can be expressed as follows:

$$\begin{aligned} c_{ij}(\xi)u_j(\xi, \omega) + \int_S [t_{ij}^*(\xi, x, \omega)_{\text{DYN}} - t_{ij}^*(\xi, x)_{\text{STA}}] u_j(x, \omega)dS(x) + \\ + \int_S t_{ij}(\xi, x)_{\text{STA}}u_j(x)dS(x) = \int_S u_{ij}^*(\xi, x, \omega)_{\text{DYN}}t_j(x, \omega)dS(x) \end{aligned} \quad (4)$$

Where DYN = Dynamic, STA = Static. The integral of the difference between the dynamic and static nuclei, first one in Equation (4), does not present singularity when executed concomitantly as expressed because they have the same order in the both problems.

Algorithmically, equation (1) is implemented into a routine named `Nonsingd`, computing the integral using the Gaussian Quadrature without addressing problems related to singularity. To overcome singularity problems, there is a special routine called `Sing_de` that uses the artifice described in equation (4). By last, `Ghmatecd` is a routine developed to create both  $H$  and  $G$  matrices described in equation (2). Both `Nonsingd` and `Sing_de` are inside `Ghmatecd` routine.

### 3. Parallelization Strategies

A parallel implementation of BEM began by analyzing and modifying a sequential code provided by [Carrion 2002]. `Gprof`, a profiling tool by [GNU], revealed the two most time-consuming routines: `Ghmatecd` and `Nonsingd`, with 60.9% and 58.3% of the program total elapsed time, respectively. Since most calls to `Nonsingd` were from `Ghmatecd`, most of the parallelization effort was focused on that last routine.

#### 3.1. Ghmatecd Parallelization

Algorithm 1 shows the pseudocode of `Ghmatecd` subroutine. Let  $n$  be the number of mesh elements and  $m$  the number of boundary elements. `Ghmatecd` builds matrices  $H$  and  $G$  by computing smaller  $3 \times 3$  matrices returned by `Nonsingd` and `Sing_de`.

---

**Algorithm 1** Creates  $H, G \in \mathbb{C}^{(3m) \times (3n)}$

---

```

1: procedure GHMATECD
2:   for  $j := 1, n$  do
3:     for  $i := 1, m$  do
4:        $ii := 3(i - 1) + 1; jj := 3(j - 1) + 1$ 
5:       if  $i == j$  then
6:          $Gelement, Helement \leftarrow \text{Sing\_de}(i)$   $\triangleright$  two  $3 \times 3$  complex matrices
7:       else
8:          $Gelement, Helement \leftarrow \text{Nonsingd}(i, j)$ 
9:        $G[ii : ii + 2][jj : jj + 2] \leftarrow Gelement$ 
10:       $H[ii : ii + 2][jj : jj + 2] \leftarrow Helement$ 

```

---

There is no interdependency between all iterations in lines 2-3 loops, thus, all iterations can be computed in parallel. Since typically high-end CPUs have 8 cores, even a small number of mesh elements generate enough workload to use all CPUs resources if this strategy alone is used. On the other hand, a GPU contain thousands of processors, hence even a considerable large amount of elements may not generate a workload in a way that it consumes all the device's resources. Since `Nonsingd` is the cause of the high time cost of `Ghmatecd`, the main effort was to implement an optimized version of `Ghmatecd`, called `Ghmatecd_Nonsingd`, that only computes the `Nonsingd` case in the GPU, and leave `Sing_de` to be computed in the CPU after the computation of `Ghmatecd_Nonsingd` is completed. The pseudocode in Algorithm 2 pictures a new

strategy where Nonsingd is also computed in parallel. Let  $g$  be the number of Gauss quadrature points.

---

**Algorithm 2** Creates  $H, G \in \mathbb{C}^{(3m) \times (3n)}$

---

```

1: procedure GHMATECD_NONSINGD
2:   for  $j := 1, n$  do
3:     for  $i := 1, m$  do
4:        $ii := 3(i - 1) + 1; jj := 3(j - 1) + 1$ 
5:       Allocate Hbuffer and Gbuffer, buffer of matrices  $3 \times 3$  of size  $g^2$ 
6:       if  $i \neq j$  then
7:         for  $y := 1, g$  do
8:           for  $x := 1, g$  do
9:              $Hbuffer(x, y) \leftarrow \text{GenerateMatrixH}(i, j, x, y)$ 
10:             $Gbuffer(x, y) \leftarrow \text{GenerateMatrixG}(i, j, x, y)$ 
11:             $Gelement \leftarrow \text{SumAllMatricesInBuffer}(Gbuffer)$ 
12:             $Helement \leftarrow \text{SumAllMatricesInBuffer}(Hbuffer)$ 
13:             $G[ii : ii + 2][jj : jj + 2] \leftarrow Gelement$ 
14:             $H[ii : ii + 2][jj : jj + 2] \leftarrow Helement$ 
15: procedure GHMATECD_SING_DE
16:   for  $i := 1, m$  do
17:      $ii := 3(i - 1) + 1$ 
18:      $Gelement, Helement \leftarrow \text{Sing\_de}(i)$ 
19:      $G[ii : ii + 2][ii : ii + 2] \leftarrow Gelement$ 
20:      $H[ii : ii + 2][ii : ii + 2] \leftarrow Helement$ 
21: procedure GHMATECD
22:   Ghmatedcd_Nonsingd()
23:   Ghmatedcd_Sing_de()
```

---

The Ghmatedcd.Nonsingd can be implemented as a CUDA kernel. Inside of a CUDA block, there are created  $g \times g$  threads to compute in parallel the two nested loops in lines 2-3 and allocate spaces in the shared memory to keep the buffer of matrices (*Hbuffer* and *Gbuffer*). Since these buffers contain matrices of size  $3 \times 3$ , nine of these  $g \times g$  threads can be used to sum all matrices because one thread can be assigned to each matrix entry, unless  $g < 3$ . Notice that  $g$  is also upper-bounded by the amount of shared memory available in the GPU. Launching  $m \times n$  blocks to cover the two nested loops in lines 2 to 3 will generate the entire  $H$  and  $G$  without the Sing\_de part. The Ghmatedcd\_Sing\_de can be parallelized with a simple OpenMP Parallel for clause, and it will calculate the remaining  $H$  and  $G$ .

#### 4. Methods

In order to check if the final result obtained by the parallel program is numerically compatible with the original, the concept of matrix norms are necessary. Let  $A \in \mathbb{C}^{m \times n}$ . [Watkins 2004] defines matrix 1-norm as:

$$\|A\|_1 = \max_{1 \leq j \leq n} \sum_{i=1}^m |a_{ij}| \quad (5)$$

**Table 1. Data experiment set**

Number of Mesh elements	240	960	2160	4000
Number of Boundary elements	100	400	900	1600

All norms have the property that  $\|A\| = 0$  if and only if  $A = 0$ . Let  $u$  and  $v$  be two numerical algorithms that solve the same problem, but in a different way. Let now  $y_u$  be the result computed by  $u$  and  $y_v$  be the result computed by  $v$ . The *error* between these two values can be measured computing  $\|y_u - y_v\|$ . The error between CPU and GPU versions of  $H$  and  $G$  matrices were computed by calculating  $\|H_{cpu} - H_{gpu}\|_1$  and  $\|G_{cpu} - G_{gpu}\|_1$ . An automated test check if this value is bellow  $10^{-4}$ .

Gfortran 5.4.0 [GFortran 2017] and CUDA 8.0 [NVIDIA 2017] were used to compile the application. The main flags used in Gfortran are `-Ofast -march=native -funroll-loops -flto`. The flags used in CUDA nvcc compiler are: `-use-fast-math -O3 -Xptxas --opt-level=3 -maxrregcount=32 -Xptxas --allow-expensive-optimizations=true`.

For experimenting, there were four data samples as illustrated in Table 1. The application was executed for each one of the samples using the original code (serial implementation), the OpenMP version and the CUDA and OpenMP together. All tests but the sequential set the number of OpenMP threads to 4. The machine used in all experiments have an AMD A10-7700K processor paired with a GeForce GTX980<sup>1</sup>.

Before any data collection, a warm up procedure is executed, which consists of running the application with the sample three times without getting any result. Afterward, all experiments were executed 30 times per sample. Each execution produces a file with total time elapsed, where a script collected the mean and standard deviation.

GPU total time was computed by the sum of 5 elements: (1) total time to move data to GPU, (2) launch and execute the kernel, (3) elapsed time to compute the result, (4) time to move data back to main memory, (5) time to compute the remaining  $H$  and  $G$  parts in the CPU. The elapsed time was computed in seconds with the OpenMP library function `OMP_GET_WTIME`. This function calculates the elapsed wall clock time in seconds with double precision. All experiments set the Gauss Quadrature Points to 8.

## 5. Results

The logarithmic scale graphic at Figure 1 illustrates the results. All points are the mean of the time in seconds of 30 executions as described in Methodology. The average is meaningful as the maximum standard deviation obtained was 2.6% of the mean value.

The speedup acquired in the 4000 mesh elements sample with OpenMP and CUDA+OpenMP with respect to the sequential algorithm are 2.7 and 107 respectively. As a conclusion, the presented strategy paired with GPUs can be used to accelerate the overall performance of the simulation for a large number of mesh elements. This is a consequence of parallelizing the construction of both matrices  $H$  and  $G$ , and the calculations in the `Nonsingd` routine. Notice that there is a performance loss in the 260 sample

<sup>1</sup>Thanks to NVIDIA for donating this GPU.

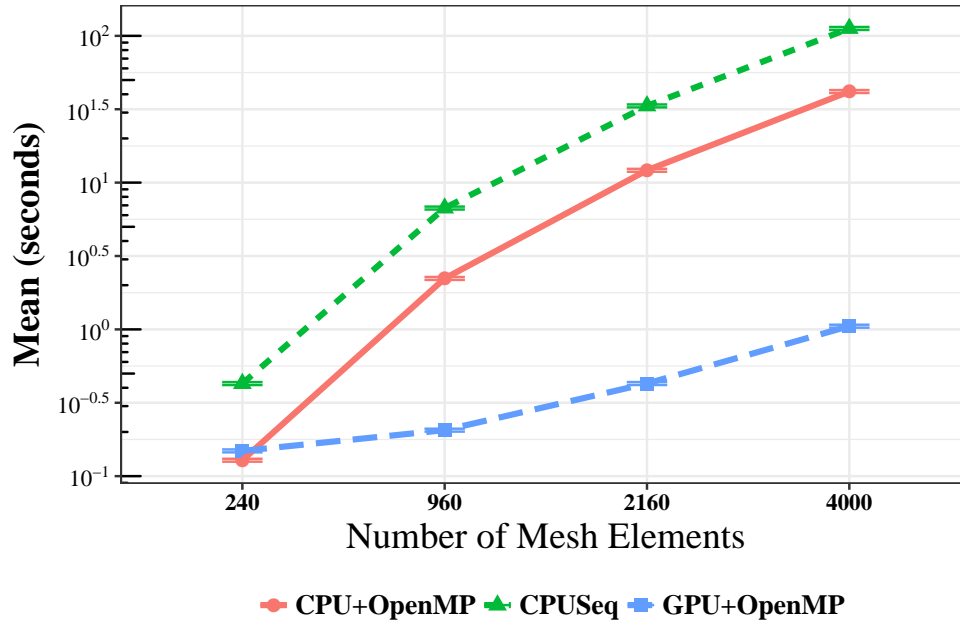


**Figure 1. Time elapsed by each implementation in logarithm scale**

between OpenMP and CUDA+OpenMP, this is caused by the high latency between CPU-GPU communication, thus the usage of GPUs may not be attractive for small meshes.

## 6. Future Work

There are some issues related to the  $g$  described in Algorithm 2. Detailed studies are required to determine the exact value of  $g$  that provides a good relation between precision and performance. Also, better ways to compute the sum in lines 11-12 of Algorithm 2 may increase performance. The usage of GPUs for the singular case can also be analyzed.

## References

- Ascher, U. M. and Greif, C. (2011). *A first course on numerical methods*. SIAM.
- Carrion, R. (2002). *Uma Implementação do Método dos Elementos de Contorno para problemas Viscoelastodinâmicos Estacionários Tridimensionais em Domínios Abertos e Fechados*. PhD thesis, Universidade Estadual de Campinas.
- Dominguez, J. (1993). *Boundary elements in dynamics*. Wit Press.
- GFortran, G. (2017). Gnu gfortran options. <https://gcc.gnu.org/onlinedocs/gfortran/Option-Summary.html>. Accessed: 2017-07-09.
- GNU. Gnu binutils. <https://www.gnu.org/software/binutils/>. Accessed: 2017-05-08.
- Katsikadelis, J. T. (2016). *The Boundary Element Method for Engineers and Scientists: Theory and Applications*. Academic Press.
- NVIDIA (2017). Cuda toolkit documentation. <http://docs.nvidia.com/cuda/cuda-compiler-driver-nvcc/>. Accessed: 2017-07-09.

Patterson, D. A. and Hennessy, J. L. (2007). Computer organization and design. *Morgan Kaufmann*.

Watkins, D. S. (2004). *Fundamentals of matrix computations*, volume 64. John Wiley & Sons.